PHYSICAL REVIEW A VOLUME 27, NUMBER 1 JANUARY 1983

Lattice of disclinations: The structure of the blue phases of cholesteric liquid crystals

S. Meiboom, M. Sammon, and W. F. Brinkman
Bell Laboratories, Murray Hill, New Jersey 07974
(Received 12 April 1982)

We argue that the basic mechanism stabilizing the blue phases is the appearance of double cholesteric twist. The free-energy cost of the disclination lattice that inevitably accompanies double twist becomes small near the clearing point. We use the director picture and the Oseen-Frank equations in a computer calculation of the free energy for three specific models, with O^5, O^2, and O^8 symmetry. Disclinations are treated as having an isotropic core. Comparison of the results of the computation with a number of experimental quantities is given. In a final section, a mean-field theory of disclinations is presented. It is argued there that the biaxiality, which is a characteristic of Landau theories of the blue phase, can be considered as an "escape" of the core of the disclination, forced by the implicit requirement of analyticity.

I. INTRODUCTION

The blue phases of cholesteric liquid crystals appear in a narrow temperature range (of the order of 1 °C) between the regular cholesteric and the isotropic phases.[1,2] Even in this narrow range a succession of two or three thermodynamically stable blue phases is often observed.[1–5] Experimentally, it is now well established that most of the blue phases have a periodic cubic structure,[3–6] with a unit-cell dimension of the order of the cholesteric pitch. An exception is a phase, variously designated as "gray phase,"[1] "blue fog,"[4] of BPIII,[5] which appears in some materials at the high end of the blue-phase temperature range. The structure of this phase is still obscure; light scattering indicates that it does not have a periodic lattice, but that it does have helical elements. In the present paper we deal with the cubic phases exclusively.

Saupe[2] was the first to suggest a cubic structure for the blue phases but presented no justification as to why such phases would become stable, relative to the helical structure, at temperatures near the clearing point (i.e., the transition to the isotropic liquid). Brazovskii *et al.*[7,8] were the first to present calculations showing how this might happen. Their treatment is based on Landau theory, and suggested a hexagonal structure. Similar theories by Alexander[9] and by Hornreich and Shtrikman[10–12] advanced cubic structures. In these theories the local order parameter is strongly biaxial.

In the present paper we discuss a somewhat different approach, an outline of which was given previously in a short communication.[13] Our model of the blue phases is based on the idea of lowering the free energy by the introduction of double twist to satisfy chirality in a symmetric fashion. It results in a lattice of disclinations, with the material between the disclinations satisfying the Oseen-Frank elastic equations. That is, we treat a director field containing a lattice of singular lines (disclinations). In contrast, the Landau theory treats a nonsingular field of a tensorial order parameter and introduces strong biaxiality. The relationship between the two treatments will be discussed in Sec. VII. It will be argued there that they can be considered as different approximations for the same basic models, and that the biaxiality can be attributed to the mean-field description of the core of the disclinations.

The organization of the paper is as follows: In Sec. II the physical basis of the theory will be discussed. In Sec. III we advance various models for which detailed calculations have been made. Section IV gives an outline of the computer program used for the energy calculations of these models. In Sec. V the results of the calculations are given and in Sec. VI these are compared with experimental results. Section VII presents a treatment of disclinations in nematic liquid crystals in the mean-field approximation. This serves as the basis for the comparison of the present theory with the Landau treatment referred to above.

II. CHIRALITY AND DOUBLE TWIST

In order to understand the reason for the existence of the blue phases, it is necessary to realize the underlying symmetry implied by chirality and its mathematical manifestation in the elastic energetics of liquid crystals. Cholesteric liquid crystals invari-

 ©1983 The American Physical Society

ably contain chiral molecules, i.e., molecules with one or more asymmetric centers. Such molecules have a built-in screw sense, and as a result they will stack in the liquid crystalline phase with their long axes at a slight angle relative to one another, rather than parallel on the average, as nonchiral molecules do. The important point is that they tend to do so for all directions of stacking perpendicular to their long axis. This is so because in the nematic and cholesteric phases the molecules rotate essentially isotropically about their long axes. To use a suggestive (though maybe not strictly accurate) simile, one can think of the molecules as screws which interleave the grooves of their threads by being at a slight angle, one relative to another. In a cholesteric with a single twist axis one has satisfied the energetics of chirality in only one direction. Consequently, one expects that at least locally there are textures which have a lower free energy than the cholesteric configuration. In order to verify that this is so, consider the elastic free-energy density in its simplest form with all elastic constants equal[14]:

$$F_e=\frac{K}{2}[(\partial_\alpha n_\beta+q_0\epsilon_{\alpha\beta\gamma}n_\gamma)^2-q_0^2] . \quad (2.1)$$

Here K is the elastic constant, α,β,γ index the coordinates, ∂_α denotes the derivative with respect to x_α, $\epsilon_{\alpha\beta\gamma}$ is the antisymmetric tensor, and q_0 is the reciprocal of the cholesteric pitch times 2π. The $-q_0^2$ term is included to make the zero of energy correspond to that usually adopted. This expression is manifestly symmetric in the plane perpendicular to the director $\vec{n}$ and consequently has the correct symmetry for chiral molecules. In fact, if one inserts in this expression a director of the form

$$\vec{n}=(1,q_0z,-q_0y) , \quad (2.2)$$

describing a local double twist, one obtains for the elastic energy $F_e(\vec{r}=0)=-(K/2)q_0^2$. Its value for the usual cholesteric, described by

$$\vec{n}=(1,q_0z,0) , \quad (2.3)$$

is zero, so that locally the normal cholesteric is of higher energy.

The F_e above is simply related to the usual Oseen-Frank expression for the elastic energy density[16]:

$$\begin{aligned}F_e=&\tfrac{1}{2}K_{11}(\vec{\nabla}\cdot\vec{n})^2+\tfrac{1}{2}K_{22}(\vec{n}\cdot\vec{\nabla}\times\vec{n}+q_0)^2\\&+\tfrac{1}{2}K_{33}[\vec{n}\times(\vec{\nabla}\times\vec{n})]^2\\&+\tfrac{1}{2}(K_{22}+K_{24})\vec{\nabla}\cdot[(\vec{n}\cdot\vec{\nabla})\vec{n}-(\vec{\nabla}\cdot\vec{n})\vec{n}] . \quad (2.4)\end{aligned}$$

By evaluating each term in this expression it is found that the term involving a total divergence contributes a $-2q_0^2$ term when Eq. (2.2) is inserted and is the source of the local energy lowering in that case. The fact that the chiral symmetry is contained in a divergence term, i.e., one that can, in principle, be converted into a surface integral, can be understood in terms of global topology—namely, that one cannot continue rotating the director along two independent directions without eventually either undoing one of the rotations, or introducing surfaces or defects in the liquid. Therefore, attempting to satisfy chirality by double twist through the volume of the liquid is not possible. Thus, we interpret all the phenomena near the cholesteric-isotropic transition—blue phases, batonnets, the blue fog, etc.—as a result of the liquid attempting locally to satisfy chirality while introducing surfaces and defects in order to satisfy global constraints. Such phenomena only occur sufficiently close to the phase transition, where the energy to create defects or isotropic regions is not prohibitive.

In the ordered cubic phases—blue phase I and II, which are the two primary phases observed—we argue that the most likely structure involves $-\frac{1}{2}$ disclinations. It is clear that an attempt to introduce point defects will not result in large contributions from the divergence term in Eq. (2.4), since when this term is reduced to a surface integral surrounding a point defect the contribution will be proportional to the radius of the core of the defect. Since this radius is expected to be of order 100 Å, one cannot expect large contributions. For line defects, however, the situation is quite different. In particular, for a $-\frac{1}{2}$ disclination we obtain the following for the energy per unit length of disclination:

$$\frac{K}{2}\int d\vec{s}\cdot[(\vec{n}\cdot\vec{\nabla})\vec{n}-(\vec{\nabla}\cdot\vec{n})\vec{n}]=-\frac{\pi}{2}K . \quad (2.5)$$

Since this result does not depend on core radius, it can give rise to a much larger contribution than point defects. One could, of course, introduce surfaces, but presumably the surface area and the large volumes of isotropic medium would be energetically unfavorable as one moves away from the transition temperature. The blue fog and other growth phenomena that occur extremely close to the isotropic phase may be the result of surfaces introduced to surround regions of double twist.

Before going on to calculate the energetics of three-dimensional periodic structures, it is instructive to consider a simple example to illustrate how the surface integral surrounding a disclination and regions of double twist are coupled. First, consider simply a $-\frac{1}{2}$ disclination in a finite system, that is, suppose

$$\vec{n}=\left[\cos\frac{\phi}{2},-\sin\frac{\phi}{2},0\right] ,$$

where ϕ is the azimuthal angle in cylindrical coordinates. If the surface integral, Eq. (2.5), is evaluated, then the integral around the core of the disclination is canceled exactly by the integral on the outside surface. However, in such a case there is no region of double twist and one does not expect to obtain a net contribution. On the other hand, consider the texture in Fig. 1. The shortened marks in the central region are to indicate an "escape" into the vertical orientation at the center. It is easily seen that, since $\vec{n}$ becomes uniform at large distances, there is no contribution to the surface integral except $-\pi K$ from the two disclinations. When the divergence term is viewed as a bulk integral, the $-\pi K$ arises from the central region of the texture, which contains considerable double twist. This example is actually a defect in a nematic and one cannot consider energetics. However, from this illustration it is clear that three-dimensional models for the blue phases should be constructed by forming cylinders containing double twist such as the central region in Fig. 1, compensated by $-\frac{1}{2}$ disclinations. Such models are discussed and evaluated in Sec. III.

III. MODELS FOR THE BLUE PHASES

Saupe was the first to propose a cubic model of the blue phases incorporating double twist and singularities. A model with the same symmetry was used by Hornreich and Shtrikman[10] and by Alexander[9] in their first papers on the Landau theory. This structure has O^5(I432) symmetry. A sketch of the unit cell is given in Fig. 2.

Other models can be made up by visualizing tubes in which the director points along the tube axis in the center, but twists away from this direction as one moves radially outward. The angle on the surface of the cylinder can be adjusted to fit cylinders together. The director field between the cylinders forms either $-\frac{1}{2}$ disclination or (escaped) $+1$ disclinations, depending on the director configuration

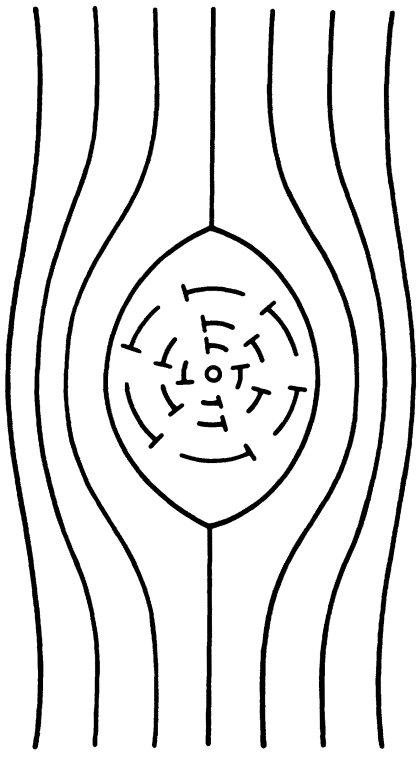

FIG. 1. Example of the relation between double twist and disclinations. Lines indicate director orientation in the plane of the figure; "nails" a tilted director; point in the center a director normal to the plane. Center part illustrates double twist; it can be thought of as an "escaped" $+1$ disclination. It is flanked by two $-\frac{1}{2}$ disclinations.

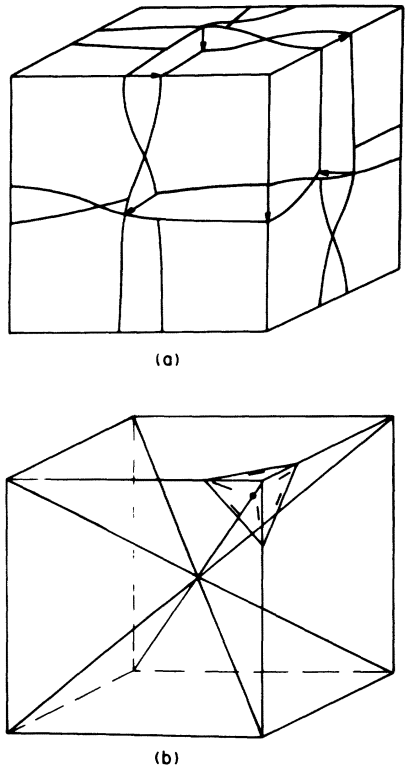

FIG. 2. Unit cell of the O^5 structure. Top figure shows the double twist. Note the reversal of the director, indicated by arrows, as one circles a body diagonal. $-\frac{1}{2}$ disclinations are along the body diagonals, as indicated in the lower figure.

on the adjacent cylinder surfaces. Sethna[13] considered a structure in which sets of cylinders were arranged parallel to the cubic axes. Such a model produces $-\frac{1}{2}$ disclinations along half of the body diagonals; see Fig. 3. This is a simple-cubic structure, of symmetry $O^2(P4_232)$.

An attractive structure has been suggested by Hornreich and Shtrikman,[11] in which four sets of tubes are arranged in the directions of the body diagonals of the unit cell along lines whose coordinates are (x,x,x), $(\frac{1}{2}+x,\frac{1}{2}-x,\bar{x})$, $(\bar{x},\frac{1}{2}+x,\frac{1}{2}-x)$, $(\frac{1}{2}-x,\bar{x},\frac{1}{2}+x)$, plus the body-centered equivalent lines. This gives a body-centered structure of $O^8(I4_132)$ symmetry. The arrangement of the disclinations we have used for the numerical calculations is sketched in Fig. 4. They run along the lines $(\frac{1}{4},0,z)$, $(x,\frac{1}{4},0)$, $(0,y,\frac{1}{4})$, plus the body-centered equivalent lines. However, it should be noted that these lines are the 4_1 axes of the O^8 group, and therefore symmetry requires only that the disclinations spiral about these lines.

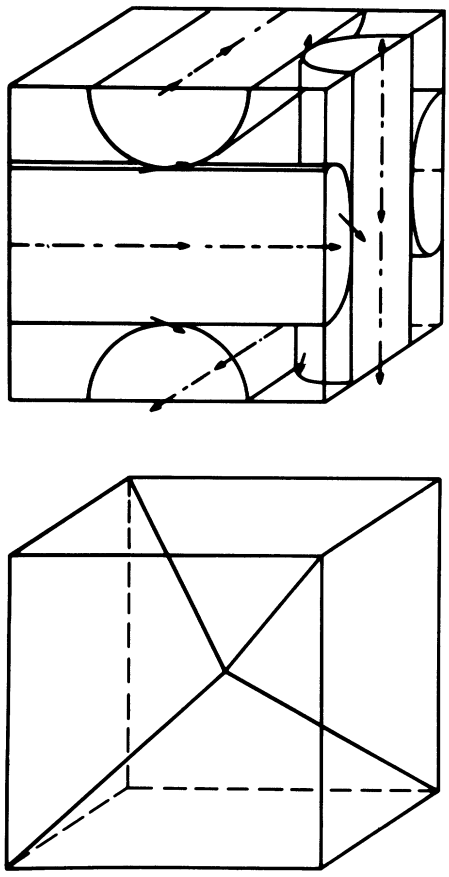

FIG. 3. Unit cell of the O^2 structure. In the cylinders the director rotates by 45° away from the axis direction on going radially out to the cylinder surface. Rotation is right handed everywhere. When following the arrows in the top figure, note that the sense reverses when traversing the upper circuit, but not when traversing the lower one. $-\frac{1}{2}$ disclinations, shown in the lower figure, are in accord with this fact. This is a simple-cubic structure; though the corners of the unit cell exhibit the same conformation of disclinations as the center, they are rotated by 90°.

For the computer calculations of the elastic energy (to be described in Sec. IV), it is crucial to have a starting trial director configuration which has the correct symmetry of the model. The numerical relaxation of this configuration will minimize the energy, but cannot change the topology of the director field. The overall symmetry of the lattice is determined by the boundary conditions on the unit cell and by the initial topology. This symmetry is preserved in the relaxation process. To obtain an initial trial function for a model of given symmetry, as well as the configuration of the disclination lines for this model, we use the following systematic procedure.

We use the mean-field solutions of Alexander[9] and of Hornreich and Shtrikman.[11] They write

$$Q_{\alpha\beta}(\vec{r}) \equiv \epsilon_{\alpha\beta} - 1/3\delta_{\alpha\beta}\epsilon \equiv \alpha \sum_n Q^n_{\alpha\beta} e^{i\vec{q}_n\cdot\vec{r}}, \tag{3.1}$$

where $\epsilon_{\alpha\beta}$ is the dielectric tensor and ϵ its trace, and q_n are the various first-order reciprocal lattice vectors of the particular lattice to be studied. The $Q^n_{\alpha\beta}$ are determined by the symmetry group. There is

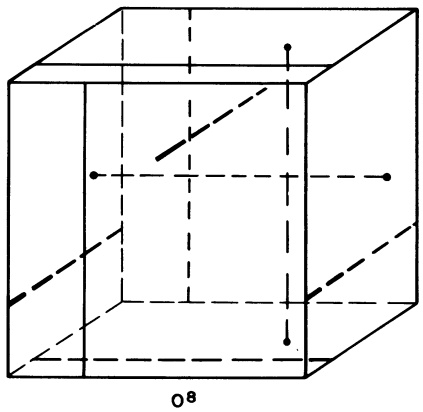

O^8

FIG. 4. Unit cell of the O^8 structure [Hornreich and Shtrikman (Ref. 11)]. Topology of this structure can be described by four sets of cylinders similar to those of Fig. 3. Axes of the cylinders are oriented parallel to the body diagonals of the unit cell. We have not tried to sketch this arrangement. Figure gives the locations in the unit cell of the resulting $-\frac{1}{2}$ disclinations.

only one set of $Q^n_{\alpha\beta}$ for a given symmetry group. $Q_{\alpha\beta}(\vec{r})$ is an analytic function of position that can be diagonalized to obtain its eigenvalues and eigenfunctions at any point in space. We choose $\vec{n}(\vec{r})$ to be the eigenfunction giving the maximum positive (prolate) eigenvalue at each point in the unit cell. This procedure is well defined except on lines where there are two degenerate maximum eigenvalues. These lines actually describe $-\frac{1}{2}$ disclinations in the structure as defined. This result is most easily seen by noting that, if one looks along a line perpendicular to the line on which the degeneracy occurs, the two eigenvalues cross, so that on moving along this perpendicular line $\vec{n}$ will suddenly change direction by 90° as required by orthogonality of the eigenfunctions. Such a change is the mark of a $\frac{1}{2}$ disclination. By careful analysis one can show they are $-\frac{1}{2}$ disclinations. As discussed in Sec. VII, this behavior is identical to a new analytic solution for the core of a $-\frac{1}{2}$ disclination.

IV. COMPUTER CALCULATIONS

The program to calculate elastic energies is a direct application of the Oseen-Frank equation, Eq. (2.4), the energy being minimized with respect to the director $\vec{n}$. Note that the surface term does not enter the variational equations, but does contribute to the total energy. As always, these equations are transformed into difference equations, with the director defined at the intersections of a three-dimensional $N\times N\times N$ mesh. Periodic boundary conditions apply on the faces of the unit cell. The computation starts with an initial director field which has a topology in accordance with the particular model being treated. The procedure to determine the starting $\vec{n}$ field and the location of the disclinations has been outlined in Sec. III.

The energy is minimized by letting the director field relax towards its equilibrium configuration. The relaxation is treated as a quasiviscous response to the torque acting on the director, the latter being the standard mean-field expression from the Oseen-Frank equation. Standard Lagrange multiplier procedure is used to satisfy the auxiliary condition that the director have unit length. To ensure stability of the solutions, the relaxation is done in small steps, and iterated until the energy stops dropping appreciably. Generally 10 to 20 iterations were sufficient.

Although the above computation procedure is straightforward, a number of aspects require elaboration. First, because the models have noninteger disclinations, it is impossible to define a global positive sense for the director field. This is illustrated in Fig. 2 by the arrows: As one follows the director around a closed path around a $-\frac{1}{2}$ disclination, the arrowhead reverses sense on each traverse of the circuit. Thus consistent director alignment can be obtained only locally. The program, in fact, checks alignment on each iteration, and reverses the director sense whenever required. If this were not done, one would overestimate the elastic energy.

A second important point is the treatment of the disclinations. Because we consider the disclinations as having an isotropic core of radius R, we wish to exclude the volume of the core from the elastic energy calculations (the core energy will be introduced separately). Moreover, we assume that on the surface of the core the director reorients under the elastic torques exerted by material outside the core only, i.e., the core interface as such exercises no orienting torque. This situation is realized in the program by the following procedure: In calculating the torque on the director at a specific mesh point, we consider the eight mesh cubes immediately surrounding the point. For each cube we calculate the change of elastic energy with the change of central director orientation; i.e., its contribution to the director torque. However, we exclude from this calculation every mesh cube which has any corner on a disclination. We also exclude these mesh cubes from the calculation of the elastic energy.

A corollary of this procedure is that the mesh size adoped for the calculation also determines an effective radius of the disclination core. In fact, we shall simply take the mesh size, written as d/N, as the effective disclination radius (here d is the size of the unit cell, and N the number of divisions along each axis of the mesh).[17] One objection to this procedure could be that N determines the mesh size, and thus the accuracy of the difference approximation. To evaluate this factor, we have made a computation with $N=24$, in which the effective core radius was doubled by excluding not only mesh cubes which touched the disclination lines, but also those that were once removed. This computation gave for the elastic energy density, Eq. (2.4), with all elastic constants equal to 3×10^{-7} dyn, the value $F_e=-0.3376\times10^4$ erg cm^{-3}. The corresponding value for the regular computation with $N=12$ produced $F_e=-0.3381\times10^4$ erg cm^{-3}. (For reference, these numbers apply to the point for $d=1.5\times10^{-5}$ cm in Fig. 6.) It can be concluded that a mesh of $N=12$ gives already ample precision.

Actual computations were made for N values up to 24, and on occasion 26. Larger N's become impractical, because of the rapidly increasing computation time and memory requirements, even on the Cray-1 computer, on which most of the computations were made. It is, however, simple to calculate

energy values for larger N's. As N increases, the radius of the disclination core becomes small compared to the pitch, and thus near the disclination the director configuration can be approximated by the one for a $-\frac{1}{2}$ disclination. The elastic energy per unit length for such a disclination, integrated between radii R_1 and R_2, is[18]

$$F_e=\frac{\pi K}{4}\ln(R_2/R_1)\,, \tag{4.1}$$

where it is assumed that $K_{11}=K_{33}\equiv K$. Using $R_1=d/N_1$ and $R_2=d/N_2$, we have

$$F_e(N_1)=F_e(N_2)+\frac{\pi K}{4}\ln(N_1/N_2)\,. \tag{4.2}$$

In Figs. 5–12 the curves with N's larger than 24 or 26 have been calculated from those for $N=24$ or 26, using the above equation. As a check, we show in Fig. 7 values for $N=24$ calculated from those for $N=20$. Although the agreement is not perfect, it seems satisfactory in view of the fact that the approximation should become better as N increases.

V. NUMERICAL RESULTS

The results of the calculations are given in graphical form in Figs. 5–10. The curves in the left half of each figure give the computer results for the elastic energy density F_e plotted against the reciprocal of the unit-cell dimension $1/d$. This elastic energy includes the splay, twist, bend, and divergence terms, and applies to the ordered region outside the disclination cores. The various curves are labeled by the value of N, the number of divisions used in the numerical integration. As explained in Sec. IV, N determines the effective radius of the disclination core as d/N.

We equate the elastic energy of the ordered region to its free energy. This can be done because any other contribution to the free-energy difference between helical cholesteric and the ordered material of the blue phase must be due to changes in the magnitude of the order parameter induced by the elastic deformation. The contribution will be of order $(\xi_0/d)^2$ compared to the elastic terms, i.e., about 1% (here

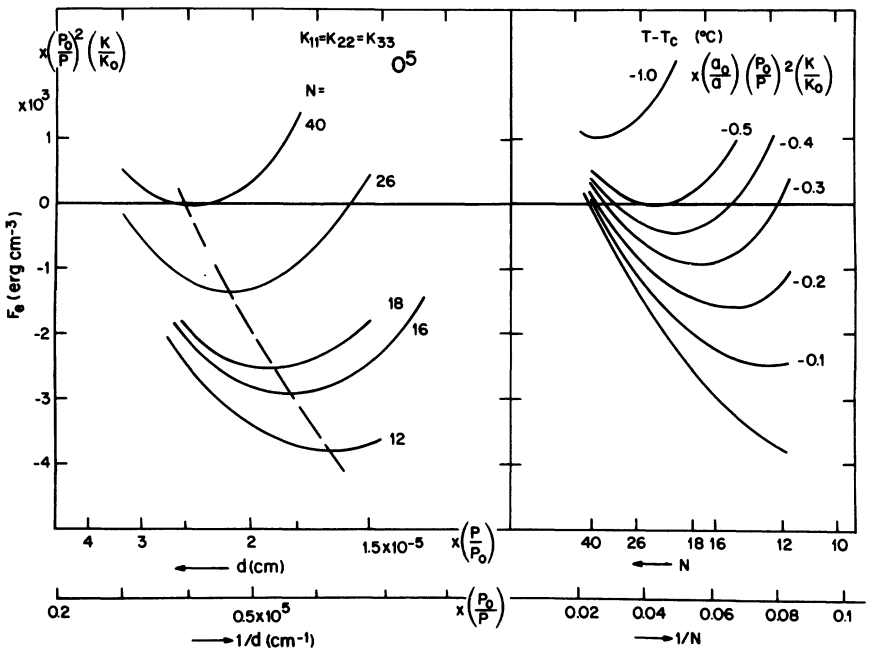

FIG. 5. Free-energy curves for the O^5 structure for the case of equal elastic constants. Curves in the left graph give the computed elastic energy density F_e as function of the lattice constant d, and do not include the energy of the disclination cores. Radius of the latter is given by d/N, as explained in the text. Curves in the right graph give the energy density when the core free energy is included, plotted as a function of N. Parameter $T-T_c$ is the temperature relative to the clearing point T_c. Because the core contribution depends on N, but not on d [Eq. (5.1)], it is sufficient to draw the curves for the values of d which minimize the free energy, i.e., the minima of the curves in the left part of the figure. Stable states are given by the minima of the curves in the right-hand side. Construction to find the corresponding lattice parameter is given in Fig. 7. Parameters used are as follows: $K_{11}=K_{22}=K_{33}=K_0=3\times10^{-7}$ dyn; cholesteric pitch, $P_0=2.5\times10^{-5}$ cm; entropy of transition $a_0=8\times10^4$ erg cm^{-3} K^{-1}. Scaling factors to be applied to the d, F_e, and $T-T_c$ scales for other parameter values are indicated in the graph.

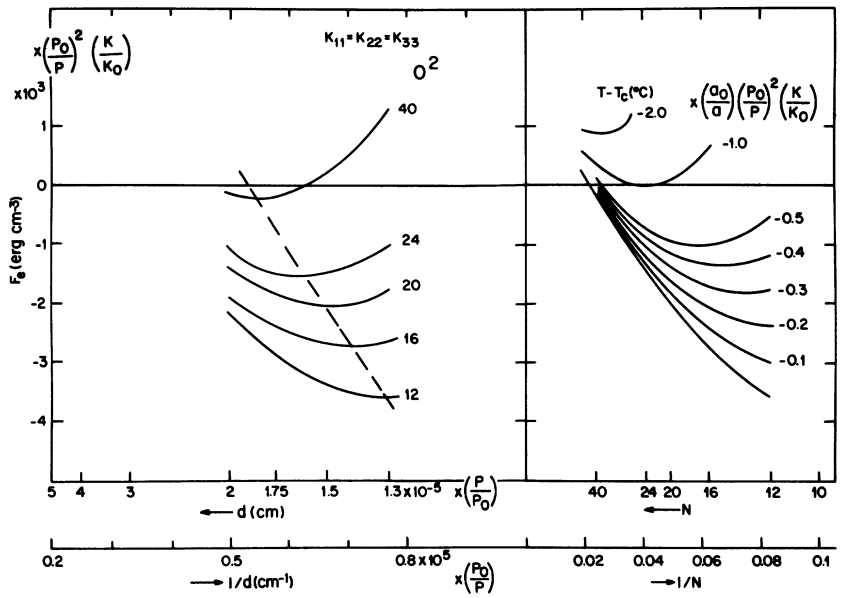

FIG. 6. Free-energy curves for the O^2 structure for the case of equal elastic constants. Other details as for Fig. 5.

ξ_0 is the coherence length; see Sec. VII.) This estimate may fail near the disclination cores, where distortions are extreme. However, such a contribution is approximately accounted for as part of a surface energy at the core interface, as introduced below.

To obtain the total free-energy density, the energy of the disclination cores has to be added. No rigorous theory of disclination cores is available.

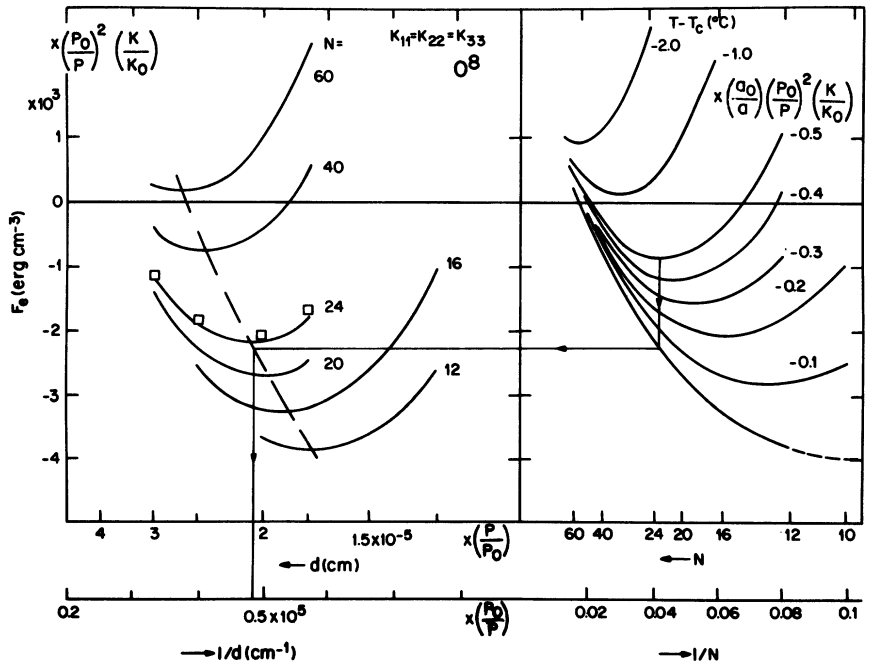

FIG. 7. Free-energy curves for the O^8 structure for the case of equal elastic constants. Other details as for Fig. 5. Arrowed lines illustrate the construction for obtaining the lattice parameter for the minimum free-energy state at $T_c-0.5$ °C. Four points indicated by squares give values for $N=24$ calculated from corresponding ones for $N=20$.

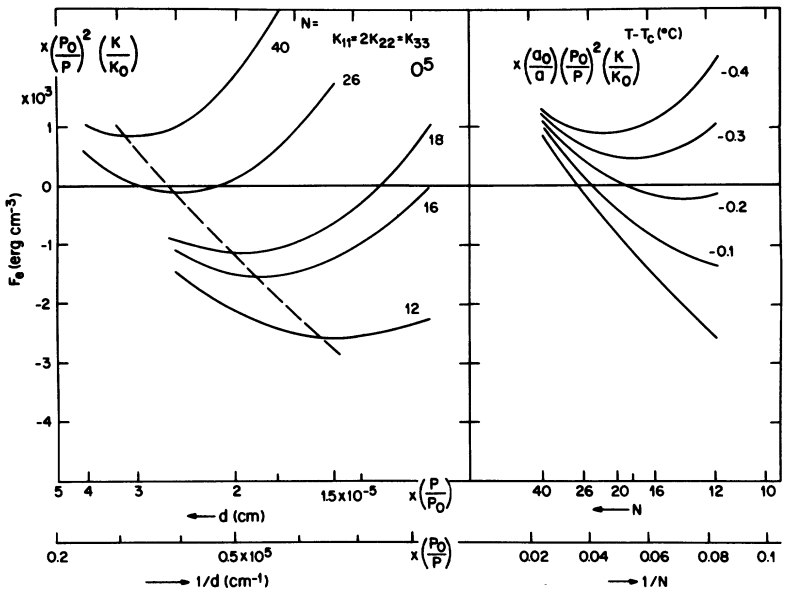

FIG. 8. Free-energy curves for the O^5 structure for the case $K_{11}=2K_{22}=K_{33}=K_0=3\times10^{-7}$ dyn. Other details as for Fig. 5.

We shall here consider three simple models. (1) An isotropic core whose free energy is given by the difference in free energy between isotropic and cholesteric material is considered first. (2) Later in this section we shall show how the addition of a surface term, accounting for an interface energy between the isotropic core and the cholesteric, influences the results. (3) A mean-field theory of disclinations will be given in Sec. VII.

At a temperature T close to the first-order transition at T_c, the difference in free energy between the isotropic and cholesteric phases is given by $a(T_c-T)$, where a is the entropy of transition.[19] Taking the O^8 structure as an example, the core

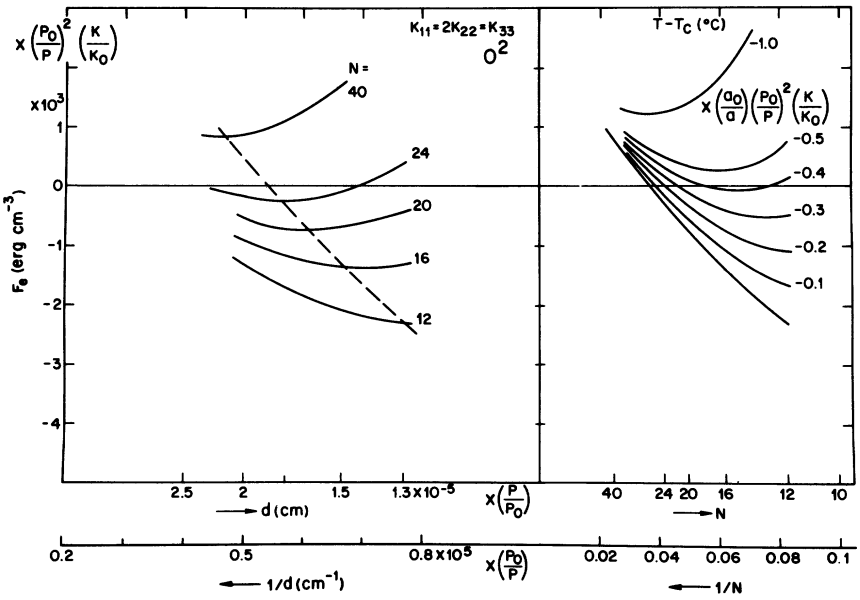

FIG. 9. Free-energy curves for the O^2 structure for the case $K_{11}=2K_{22}=K_{33}=K_0=3\times10^{-7}$ dyn. Other details as for Fig. 5.

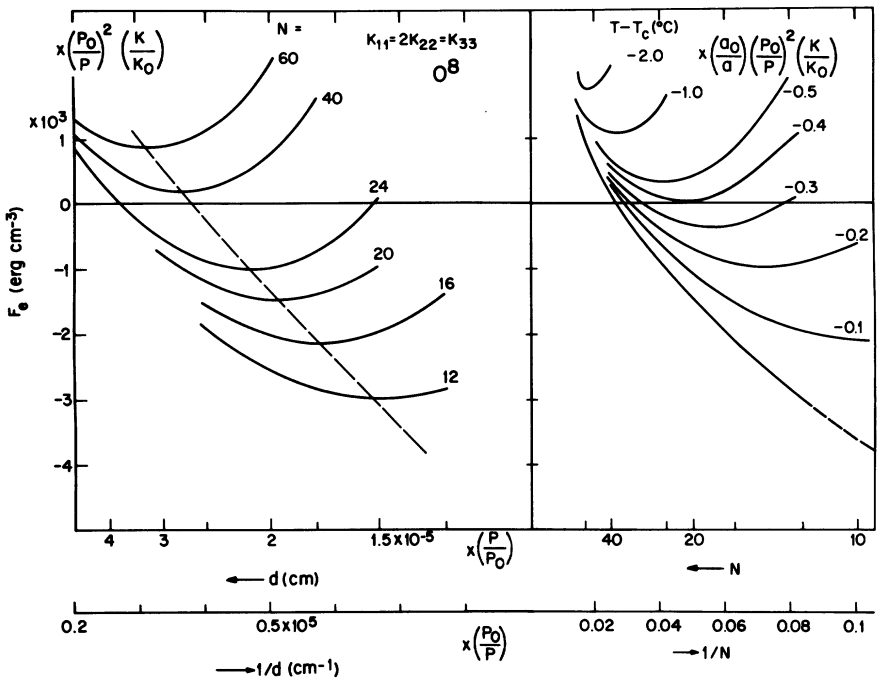

FIG. 10. Free-energy curves for the O^8 structure for the case $K_{11}=2K_{22}=K_{33}=3\times10^{-7}$ dyn. Other details as for Fig. 5.

contribution to the free-energy density is

$$F_{\text{core}}=a(T_c-T)V$$
$$=a(T_c-T)(6d\pi R^2)/d^3$$
$$=a(T_c-T)6\pi/N^2\,, \tag{5.1}$$

where V is the core volume per cm^3 of material, and $R=d/N$ the effective core radius. $6d$ is the length of the disclinations in the O^8 unit cell.

We are interested in the minimum of the total free energy, taking d and N as variables, at a constant

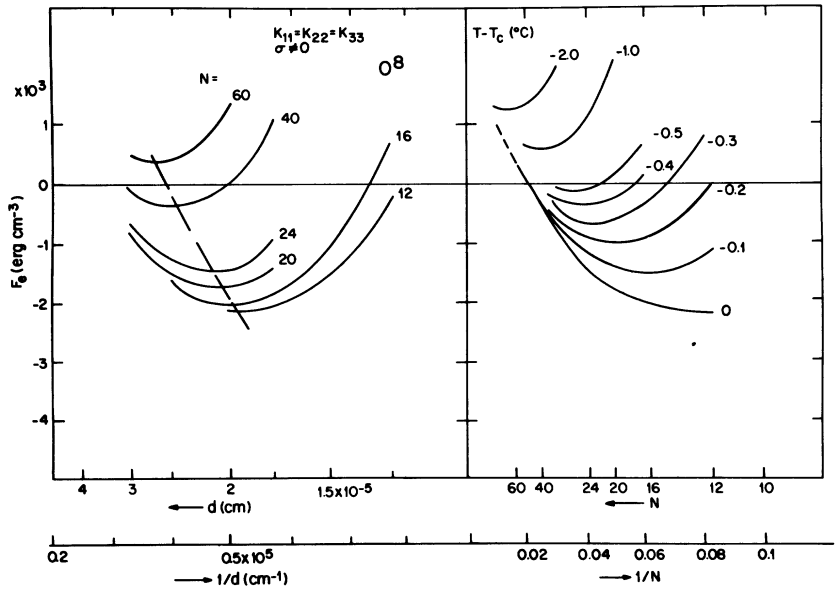

FIG. 11. Free-energy curves for the O^8 structure for the case of equal elastic constants. A surface-energy term for the isotropic-cholesteric interface has been added. A surface tension of $\sigma=1\times10^{-2}$ erg cm^{-2} has been used in the calculations. Other details as for Fig. 5, except that scaling does not apply here.

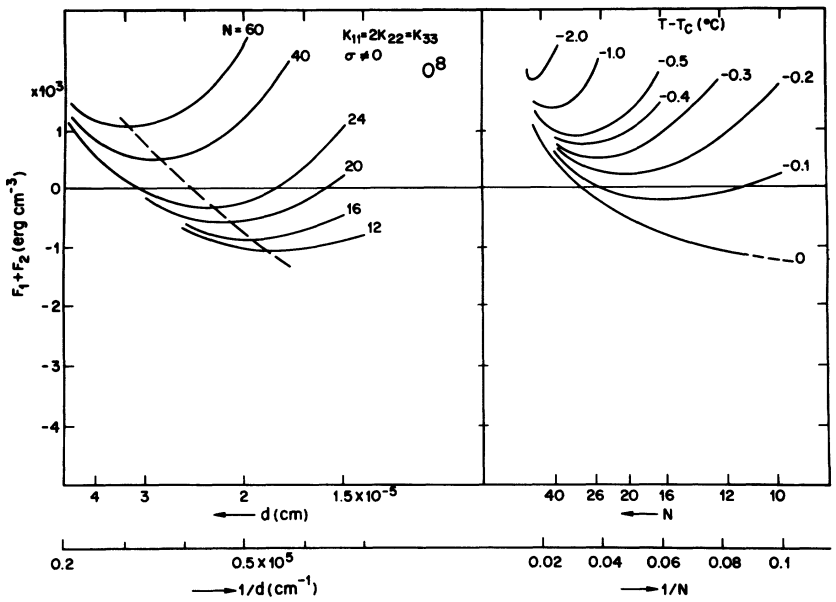

FIG. 12. Free-energy curves for the O^8 structure for the case $K_{11}=2K_{22}=K_{33}=3\times10^{-7}$ dyn. Other details as for Fig. 11.

temperature. Because the expression for F_{core}, Eq. (5.1), does not depend on d, we need only consider the minima of the F_e vs d curves. Thus, taking Fig. 7 as an example, we plotted the minima of F_e as function of $1/N$ as the lower curve in the right half of the figure. We then add F_{core} [Eq. (5.1) for O^8] for a number of temperatures, obtaining the set of curves in the right half of the figure. The curves are labeled by the temperature, in °C below the clearing point T_c. The minima of these curves represent the stable states.

A number of conclusions can be drawn from the figure. For instance, it shows that the O^8 structure will become stable relative to the planar cholesteric (which has a free energy equal to 0 for the energy scale used) at a temperature about 0.95 °C below T_c. As the temperature increases, the minimum of the curves shifts to smaller N; the corresponding lattice constant d also decreases. The construction to obtain the latter is illustrated for the $T-T_c=-0.5$ curve by the vertical and horizontal lines marked with arrows.

Some remarks on the values of the variables used in the computations are in order. The numbers on the coordinate axes of Figs. 5 , 6, and 7 apply for elastic constants $K_{11}=K_{22}=K_{33}=3\times10^{-7}$ dyn, a cholesteric pitch $P_0=2.5\times10^{-5}$ cm, and an entropy of transition of $a=8\times10^4$ erg cm^{-3}K^{-1}. We always take $K_{22}+K_{24}=(K_{11}+K_{22})/2$, a relation which can be derived from rather general assumptions.[16] A perusal of Eqs. (2.4) and (5.1) shows that it is a simple matter to scale the results for other values, provided the ratios of the various K's remain the same. We denote the new pitch by P, a new representative elastic constant by K, the new entropy of transition by a, and the corresponding original values, as specified above, by P_0, K_0, and a_0. Then the curves will apply to the new values if the numbers on the energy scale are multiplied by $(P_0/P)^2(K/K_0)$, those on the d scale by P/P_0, and values of the temperature parameter by $(a_0/a)(P_0/P)^2(K/K_0)$. (Note that it is the numerical values that must be multiplied, not the symbols.)

The assumption of equal elastic constants, though simplifying theory considerably, is often not a good approximation for actual materials. In particular, K_{22} is generally smaller than K_{11} and K_{33}.[20] As K_{22} is a crucial parameter in the present theory, we have explored its influence by recalculating the various graphs for the case $K_{22}=K_{11}/2=1.5\times10^{-7}$ dyn; all other parameters are unchanged. The results are given in Figs. 8, 9 , and 10. As expected, the temperature range of stability of the blue phases is somewhat reduced.

The effect of introducing an interface energy is illustrated in Figs. 11 and 12 for the O^8 structure (the other structures give similar results). The contribution to the energy density can be written

$$F_{\text{int}}=\sigma(6d2\pi R)/d^3 = \sigma(12\pi)/Nd\ , \tag{5.2}$$

where σ is the surface tension, and the other quantities are defined following Eq. (5.1).

We have found only two values for σ in the literature. Kahlweit and Ostner[21] give an estimate of 5×10^{-4} erg cm^{-2} as a lower limit for *p*-azoxyphenetole. But their method of measurement (rate of coalescence of nematic droplets in an isotropic environment) does not preclude a much larger value. Langevin and Bouchiat[22] give a value of $(2.3\pm0.4)\times10^{-2}$ erg cm^{-2} for MBBA (methoxybenzylidene-butylaniline), determined from light scattering measurements. We have, arbitrarily, used a value of $\sigma=1\times10^{-2}$ erg cm^{-2} in drawing Figs. 11 and 12, which apply to identical parameters as Figs. 7 and 10, respectively, except for the introduction of the additional term, Eq. (5.2). It is seen that for this value of σ a stable blue phase persists. On the other hand, the Langevin and Bouchiat value would just about eradicate the blue phase. At present we lack the knowledge to elucidate this issue: We just do not have anything approaching a complete set of experimental parameters (σ,K's,a) for any one substance. It is our hope and belief, partly based on the results described in Sec. VI, that the interface energy does not play a decisive role in the energetics.

VI. COMPARISONS WITH EXPERIMENT

Here we discuss some observations on the blue phase taken from the literature, and compare them with the predictions of the present theory. We can only expect qualitative, or at best semiquantitative agreement, since, as already pointed out, we do not have a complete set of parameters for any one substance. Moreover, at this stage we do not know which structure corresponds to a specific observed phase.

1. Temperature dependence of the lattice constant. For all the cases shown in Figs. 5—12 the lattice constant d decreases with increasing temperature (the procedure to obtain d is indicated in Fig. 7 by the arrowed vertical and horizontal lines). In Fig. 13 we have plotted two sets of experimental values for the wavelength λ of the first Bragg reflection, which is of course proportional to the lattice constant. The first set, indicated by open circles, is from Ref. 5, and applies to cholesteryl nonanoate with 15% cholesteryl chloride. The second set, indicated by open squares, is from Ref. 1 and applies to cholesteryl benzoate. Both sets include a supercooled blue-phase region. For comparison, the figure also presents a number of calculated curves. All are for the O^8 model (the other models give comparable results), and curves for both the $K_{11}=K_{22}=K_{33}$ and $K_{11}=2K_{22}=K_{33}$ cases are given. The curves are constructed by reading off the lattice constant d as function of temperature from Figs. 7 and 10, respectively. The constant of proportionality to convert d into the Bragg reflection wavelength λ is chosen to make experimental and calculated curves coincide at the rightmost experimental point. The temperature $(T-T_c)$ has been scaled by the factor $(a_0/a)(P_0/P)^2$, as defined in Sec. V. Values used are as follows: for the cholesteryl nonanoate mixture $a=2.76\times10^4$ erg cm^{-3}K^{-1} (Ref. 1), $P=280$ nm (Ref. 5, assuming a refractive index of 1.5); for cholesteryl benzoate $a=3.24\times10^4$ erg cm^{-3}K^{-1} (Ref. 19), $P=217$ nm (Ref. 1, refractive index 1.5). We were unable to scale for the elastic constant K, as no values for the compounds involved are available. The calculated curves so obtained are indicated in Fig. 13 by the full circles and triangles for the cholesteryl nonanoate and by diamonds and inverted triangles for cholesteryl benzoate.

The pronounced flattening off with falling temperature of the curve for cholesteryl nonanoate is not well reproduced in the calculations. Some of

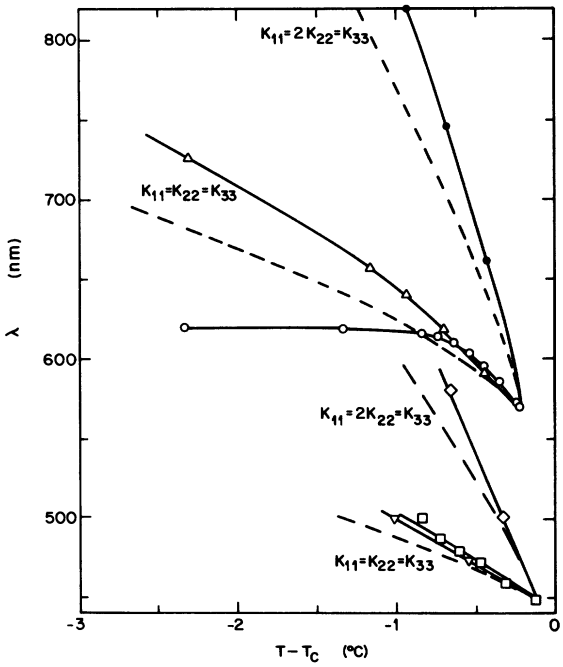

FIG. 13. Wavelength of first Bragg reflection in the BPI as a function of temperature. Curve indicated by open circles is experimental from Ref. 5 and applies to cholesteryl nonanoate-cholesteryl chloride mixture. Curve with squares is from Ref. 1, and applies to cholesteryl benzoate. Other curves are calculated for the O^8 structure, with elastic constants as indicated in the figure. Full curves are for temperature-independent elastic constants, while for the dashed curves a temperature dependence has been introduced. See Sec. VI for details.

this discrepancy might be due to the variation of the elastic constants with temperature: Very near the clearing point T_c the elastic constants vary rapidly with temperature, for nematics their values about double for a 3 °C drop.[20] Although we have no measurements for the compounds involved, we believe this behavior may be typical for nematics and cholesterics. When such a variation is taken into account, we obtain the dashed curves in Fig. 13.

2. Enthalpy of the cholesteric-blue-phase transition. We refer to experimental values given by Stegemeyer and Bergmann.[1] They are for cholesteryl myristate: cholesteric-BPI transition, 34 J mole^{-1}; blue-phase-isotropic, 1100 J mole^{-1}. The values for cholesteryl nonanoate are as follows: cholesteric-BPI, 17 J mole^{-1}; blue-phase-isotropic, 530 J mole^{-1}. We can calculate values for the cholesteric-blue-phase transition by taking the volume of the disclination cores per unit volume of material at the transition, and multiplying it with the enthalpy of the cholesteric-isotropic transition. Taking again the O^8 structure as an example, we have for the core volume per cm^3 material

$$V_{\text{core}}=\pi R^2\frac{6d}{d^3}=\frac{6\pi}{N^2}\ . \tag{6.1}$$

For the case of equal K's we find from Fig. 7 that at the transition $1/N=0.032$. Thus for cholesteryl myristate we find $\Delta H=(6\pi/N^2)1100=21.1$ J mole^{-1}. For the case $K_{11}=2K_{22}=K_{33}$ (Fig. 10) we have $1/N=0.048$ and $\Delta H=47.8$ J mole^{-1}. The corresponding figures for cholesteryl nonanoate are 10.2 and 23.0 J mole^{-1}, respectively.

In the above estimates we have neglected the change in elastic energy at the transition. An upper estimate for the elastic energy is $\frac{1}{2}Kq_0^2$. With $K=3\times10^{-7}$ dyn, a pitch $=2.5\times10^{-5}$ cm$=2\pi/q_0$, and a molecular weight of 597 for cholesteryl myristate, we obtain 0.56 J mole^{-1}, which is quite negligible.

3. Density of the blue phase. Experimental values for cholesteryl myristate have been published by Demus *et al.*[23] In Fig. 14 the full circles indicate the results from that paper.[24] To obtain a calculated value for the density, we again consider the blue phase as consisting of a fraction f_c of cholesteric material and a fraction f_i of isotropic material in the cores. Again taking the O^8 structure, we have $f_i=1-f_c=6\pi/N^2$. One can readily show that for this model the density ρ is given by

$$\rho=\rho_0\left[1-(f_c\alpha_c+f_i\alpha_i)t-f_i\frac{\Delta\rho}{\rho_0}\right], \tag{6.2}$$

where α_c and α_i are the coefficients of expansion for the cholesteric and isotropic, respectively, ρ_0 the density at the cholesteric-blue-phase transition, t the temperature measured from that transition, and $\Delta\rho$ the change in density at the (extrapolated) cholesteric-isotropic transition. The results of applying Eq. (6.2) to the O^8 structure are given in Fig. 14. The triangles are for the $K_{11}=2K_{22}=K_{33}$ case, and the open circles for the $K_{11}=K_{22}=K_{33}$ case.[25] It should be noted that, although Demus *et al.* state in their paper that they find no density discontinuity at the cholesteric-blue-phase transition, their Fig. 3 does seem to show a small jump, which we have attempted to reproduce in our Fig. 14, and which can be estimated at about 0.3×10^{-4} g cm^{-3}. The calculated values for the two cases are 0.8×10^{-4} and 0.35×10^{-4}, respectively.

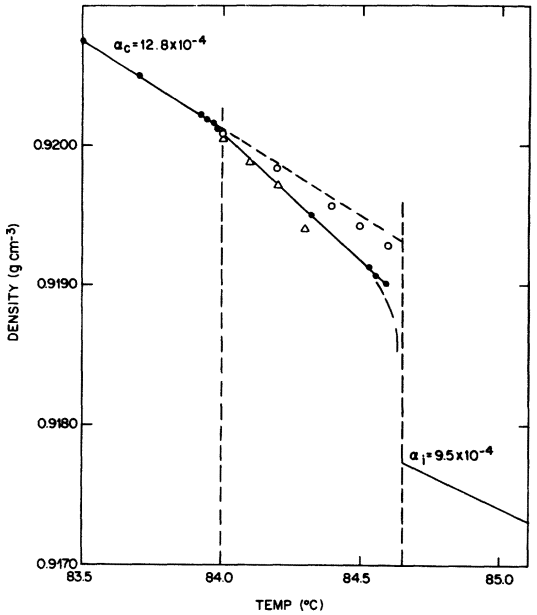

FIG. 14. Density variation with temperature of the cholesteric, blue, and isotropic phases. Full circles and lines give experimental values from Ref. 23. Triangles and open circles give calculated values for the O^8 structure for, respectively, the $K_{11}=2K_{22}=K_{33}$ and $K_{11}=K_{22}=K_{33}$ cases.

4. Dependence of the temperature range of the blue phase on pitch. It has already been remarked that in Figs. 5—10 the temperature scales with pitch as $(P_0/P)^2$. One way to investigate the validity of this relation is to plot the temperature range over which the blue phase is stable for a series of mixtures with varying pitch. Such measurements have been published by Stegemeyer and Bergmann,[1] and by Marcus and Goodby.[26] The first authors use mixtures of cholesteryl myristate and nematogenic PCPB [*p*-pentylphenyl-2-chloro-4-(*p*-pentylbenzoyloxy)-benzoate]. In Fig. 15 we have plotted the

width of the BPI and BPII region in their phase diagram as function of $1/\lambda$ (the open circles in the figure). Here λ is the wavelength of the selective reflection in the cholesteric phase, which is proportional to the pitch. For comparison we have plotted a $1/\lambda^2$ curve, normalized so as to fit the rightmost experimental point. At short pitches (large $1/\lambda$) its slope fits the experimental points remarkably well, but at long pitches the simple scaling obviously fails.

A weak point of the above measurements is that the mixture is made up of two very dissimilar compounds, and thus the relevant parameters (K's, a) may well vary with composition. To minimize such effects, Marcus and Goodby[26] have investigated mixtures of the chiral and racemic forms of the same compound [terephtaloyloxy-bis-4-(2'-methylbutyl)benzoate]. Their results are plotted as triangles in Fig. 15, and again a $1/\lambda^2$ curve is given for comparison. Here the situation is complicated by the fact that, unexpectedly, there is a BPI to BPII transition with changing composition.

The inclusion of an interface energy σ has the effect of making the blue phases unstable relative to the planar cholesteric beyond a given critical pitch. It is convenient to approximate curves for the elastic energy by an analytic function, as follows:

$$F_{\text{elas}}=K\left[\frac{A_0}{d_1^2}-\frac{1}{dd_1}+\frac{A_2}{d^2}+\frac{3\pi}{2d^2}\ln N\right]. \quad (6.3)$$

Here A_0, A_2, and d_1 are parameters which are adjusted to fit the computed curves. For the O^8 curves in Fig. 7, for example, we fit the $N=24$ curve with

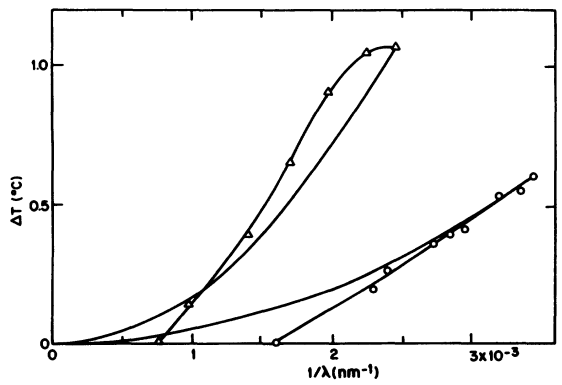

FIG. 15. Temperature range over which the blue phase is stable as a function of the wavelength of the first Bragg reflection. Curve with open circles is from Ref. 1, the one with triangles from Ref. 26. Full lines plot a c/λ^2 dependence, with c adjusted so that the right-most value fits the experimental point. Introduction of a surface energy of the disclination cores will move the latter curves down, so that a cutoff wavelength appears. See Section VI 4 for an estimate of this wavelength.

the following values: $A_0=0.0140$, $A_2=-1.14$, and $1/d_1=13.4\times10^5$ cm^{-1}. The logarithmic term expresses the dependence on N, in accordance with Eq. (4.2). Note that its coefficient as given applies to the O^8 structure, in which the disclination length per unit cell equals $6d$. (For the O^5 and O^2 structures the coefficients are $\pi\sqrt{3}$ and $\frac{1}{2}\pi\sqrt{3}$, respectively.) We now add an interface energy, Eq. (5.2), to obtain (for the O^8 case)

$$F_{\text{tot}}=K\left[\frac{A_0}{d_1^2}-\frac{1}{dd_1}+\frac{A_2}{d^2}+\frac{3\pi}{2d^2}\ln\left[\frac{d}{R}\right]+\frac{12\pi\sigma R}{d^2K}\right]. \quad (6.4)$$

We need here consider only a temperature just below T_c, as at a lower one the energy will be greater. That is, we omit the term for the core free energy. In respect to R, the expression (6.4) has a minimum for $R=K/(8\sigma)$. Thus F_{tot} is a function of d only. We solved numerically for the value $d_{\min}$ which minimizes F_{tot}, to give a value $F_{\min}$. Equation (6.4) scales with pitch as follows: A_0 and A_2 are independent of pitch, and a/d_1 scales as P_0/P. Thus it is easy to solve for various P values, and find the one (P_c) for which $F_{\min}$ becomes positive. For the O^8 structure with all K's equal and $\sigma=1\times10^{-2}$ erg cm^{-2}, we find $P_0/P_c=0.31$, or $P_c=810$ nm. This compares with the values 420 and 890 nm for the two cases of Fig. 15 (an index of refraction of 1.5 is used).

There is a notable by-product of the above treatment. It is found that for zero or small interface energy (σ) F_{tot} does not have a minimum for a positive d. This corresponds to the fact that the minimum of the curves in Figs. 5 to 10 continue to decrease as N decreases. It seems probable that this fact is related to the appearance of the blue phase III: reduction of the energy implies an unrealistic decrease of N and ultimately collapse of the periodic structure into something new. It is noteworthy, however, that a combination of nonzero interface energy σ and a long enough pitch P will produce an $F_{\min}$ at a finite d. We have calculated that for $\sigma=1\times10^{-2}$ erg cm^{-2} this occurs for pitches equal or larger than $P=P_0/0.9$.

This instability, and thus the blue phase III, would appear at P values smaller than this. In fact, it has generally been observed that the blue phase III is the first to disappear as the pitch is increased. In the phase diagram given by Marcus and Goodby,[26] the BPIII disappears at a pitch about $\frac{2}{3}$ of that of which the other blue phases disappear. The P_0/P values calculated by us, 0.9 and 0.31, would give a ratio of about $\frac{1}{3}$. However, it seems reasonable that instability would appear at a larger pitch than the

0.9 ratio indicates. For instance, a ratio of 0.8 produces stability at an N value of 3, and this is quite unrealistic for a periodic structure. A P_0/P value of 0.5, which produces stability for $N=9$, seems a reasonable guess.

VII. CORE ENERGIES AND THE LANDAU THEORY

A. Core energies

The nature of the core of a $-\frac{1}{2}$ disclination in a cholesteric should not be very different from that of a nematic liquid crystal. The typical coherence length for the magnitude of the order parameter is approximately 100 Å, while a typical cholesteric pitch is a few thousand angstroms. Therefore, we investigate this problem considering only a nematic free energy within Landau theory. In addition, we will consider all the Oseen-Frank elastic constants to be equal. Defining the order parameter

$$Q_{\alpha\beta}(\vec{r})=\epsilon_{\alpha\beta}(\vec{r})-\tfrac{1}{3}\delta_{\alpha\beta}\epsilon(\vec{r}) \tag{7.1}$$

in terms of the local tensor dielectric function, the standard free-energy density is

$$F=\frac{k}{2}\partial_\alpha Q_{\beta\gamma}\partial_\alpha Q_{\beta\gamma}+\frac{a}{2}Q_{\alpha\beta}^2-\frac{b}{3}Q_{\alpha\beta}Q_{\beta\gamma}Q_{\gamma\alpha}+\frac{c}{4}(Q_{\alpha\beta}^2)^2 . \tag{7.2}$$

Repeated indices are summed. The most general form for $Q_{\alpha\beta}$ is

$$Q_{\alpha\beta}=\bar{\alpha}(n_\alpha n_\beta-\tfrac{1}{3}\delta_{\alpha\beta})+\bar{\beta}(m_\alpha m_\beta-\tfrac{1}{3}\delta_{\alpha\beta}) . \tag{7.3}$$

The $\vec{n}$ and $\vec{m}$ are orthogonal unit vectors. If either $\bar{\alpha}$ or $\bar{\beta}$ is zero we obtain the usual nematic, while with both $\bar{\alpha}$ and $\bar{\beta}$ nonzero the order parameter is biaxial. Substituting this expression into the gradient terms in F gives

$$F_\nabla=\frac{k}{3}\{(\nabla\bar{\alpha})^2+(\nabla\bar{\beta})^2-\nabla\bar{\alpha}\cdot\nabla\bar{\beta}+3[\bar{\alpha}^2\partial_\alpha n_\beta\partial_\alpha n_\beta+\bar{\beta}^2\partial_\alpha m_\beta\partial_\alpha m_\beta+2\bar{\alpha}\bar{\beta}(m_\beta\partial_\alpha n_\beta)(n_\gamma\partial_\alpha m_\gamma)]\} , \tag{7.4}$$

while the remaining terms become

$$F_0=\frac{a}{3}(\bar{\alpha}^2+\bar{\beta}^2-\bar{\alpha}\bar{\beta})-\frac{b}{27}[2(\bar{\alpha}^3+\bar{\beta}^3)-3(\bar{\alpha}^2\bar{\beta}+\bar{\beta}^2\bar{\alpha})]+\frac{c}{9}(\bar{\alpha}^2+\bar{\beta}^2-\bar{\alpha}\bar{\beta})^2 . \tag{7.5}$$

Assuming the only temperature dependence is in the coefficient a, the transition is defined by $a_0=b^2/27c$. At that point $\bar{\alpha}=\alpha_0=b/3c$. If we define $\alpha=\bar{\alpha}/\alpha_0$ and $\beta=\bar{\beta}/\alpha_0$ and measure energies in terms of $a_0\alpha_0^2/3$ and lengths in units of the coherence length $\xi=(k/a_0)^{1/2}$, the total free energy is

$$F=(\nabla\alpha)^2+(\nabla\beta)^2-\vec{\nabla}\alpha\cdot\vec{\nabla}\beta+3[\alpha^2\partial_\alpha n_\beta\partial_\alpha n_\beta+\beta^2\partial_\alpha m_\beta\partial_\alpha m_\beta+2\alpha\beta(m_\beta\partial_\alpha n_\beta)(n_\gamma\partial_\alpha m_\gamma)]+\epsilon(\alpha^2+\beta^2-\alpha\beta)-(2\alpha^3+2\beta^3-3\alpha^2\beta-3\alpha\beta^2)+(\alpha^2+\beta^2-\alpha\beta)^2 . \tag{7.6}$$

Here $\epsilon\equiv a/a_0\cong(T-T^*)/(T_c-T^*)$. This expression must be minimized with respect to $\vec{n}$, $\vec{m}$, α, and β to obtain a solution.

The variational equations for $\vec{n}$ and $\vec{m}$ are

$$-\partial_\alpha(\alpha^2\partial_\alpha n_\beta)+\alpha\beta m_\gamma\partial_\alpha n_\gamma\partial_\alpha m_\beta-\partial_\alpha(\alpha\beta m_\beta n_\gamma\partial_\alpha m_\gamma)=\lambda n_\beta+\gamma m_\beta \tag{7.7}$$

and

$$-\partial_\alpha(\beta^2\partial_\alpha m_\beta)+\alpha\beta n_\gamma\partial_\alpha m_\gamma\partial_\alpha n_\beta-\partial_\alpha(\alpha\beta n_\beta m_\gamma\partial_\alpha n_\gamma)=\nu m_\beta+\gamma n_\beta , \tag{7.8}$$

where λ,γ,ν are Lagrange multipliers for the three auxiliary conditions $\vec{n}^2=1$, $\vec{n}\cdot\vec{m}=0$, and $\vec{m}^2=1$, respectively.

Assume $\vec{n}$ describes a $-\frac{1}{2}$ disclination in cylindrical coordinates. We take $\vec{n}=(\cos\phi/2,-\sin\phi/2,0)$ for definiteness. Assume also that $\vec{m}$ does not depend on r, the radial distance from the center of the disclination. Then if α and β only depend on r their gradients will be orthogonal to the other gradients in Eqs. (7.7) and (7.8). We have

$$\vec{m}=\left[\sin\frac{\phi}{2},\cos\frac{\phi}{2},0\right] . \tag{7.9}$$

As can be easily verified, $\vec{m}$ generates a solution to the variational equations. The resulting terms in the free energy involving the gradients of $\vec{n}$ and $\vec{m}$ become

$$F_2=\frac{3}{4}\frac{(\alpha-\beta)^2}{r^2} . \tag{7.10}$$

We have solved for the solutions to the variational equations obtained by varying

$$F=\int d^2r\left[(\nabla\alpha)^2+(\nabla\beta)^2-\vec{\nabla}\alpha\cdot\vec{\nabla}\beta+\frac{3}{4}\frac{(\alpha-\beta)^2}{r^2}\right.$$
$$+\epsilon(\alpha^2+\beta^2-\alpha\beta)$$
$$-(2\alpha^3+2\beta^3-3\alpha^2\beta-3\alpha\beta^2)$$
$$\left.+(\alpha^2+\beta^2-\alpha\beta)^2\right], \quad (7.11)$$

with respect to α and β.

At small r, $\alpha+\beta=A+A_2r^2$ and $\alpha-\beta=B_1r+B_2r^2$, while at large r, $\alpha=\alpha_\infty\equiv\frac{1}{4}[3+(9-8\epsilon)^{1/2}]$ and $\beta=0$ and the first corrections are of order $1/r^2$. The variational equations were solved using a standard software package for nonlinear differential equations written by N. L. Schryer. The results for α and β for three values of $\epsilon(1.0,0.8,0.0)$ are shown in Fig. 16. One observes that β is generally small and decreases rapidly. In fact, a variational calculation with $\beta=0$ gave total energies within a few percent of the minimum energy when β is included. In Table I we give the final result for the total energy written as

$$F=E_0+\frac{3\pi}{2}\alpha_\infty^2\ln\left[\frac{R}{r_c}\right], \quad (7.12)$$

so that r_c is determined by equating

$$\int^R d^2r\frac{3}{4}\frac{(\alpha-\beta)^2}{r^2}=\frac{3\pi}{2}\alpha_\infty^2\ln\left[\frac{R}{r_c}\right], \quad (7.13)$$

and E_0 is the contribution from the remaining terms in the free energy. The core radius clearly contracts as ϵ or temperature decreases. The variation of the core energy obtained here is very similar to that obtained by using Eqs. (4.1), (5.1), and (5.2). In fact, the results in Table I can be fitted using these equations provided temperature-dependent elastic constants are used. Since it is not clear that mean-field theory gives a good description of these energies we have chosen to study the stability of various three-dimensional structures with the simple phenomenological expression involving simple physical parameters. It should be noted that the solutions in Fig. 16 do not appear as an isotropic core with an interface between it and the nematic. Within mean-field theory including only first-order terms there is only *one* length in this problem, so that such a structure

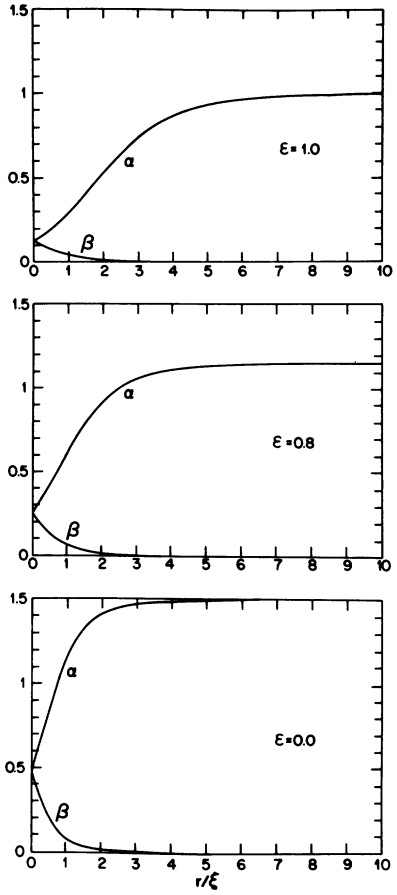

FIG. 16. Variation of order parameters with radius in the mean-field theory of a disclination. In each graph the top curve gives α, and the bottom one β; the abscissa is the radius from the center of the disclination in terms of the correlation length ξ. These quantities are defined in Eq. (7.3) and below Eq. (7.5). Temperature T is given as $\epsilon\equiv(T-T^*)/(T_c-T^*)$, where T^* is the (extrapolated) second-order transition temperature, and T_c the first-order transition temperature.

TABLE I. Numerical results from mean-field calculations.

$$F=E_0+\frac{3\pi\alpha_\infty^2}{2}\ln\left[\frac{R}{r_c}\right]$$
$$\alpha_\infty\equiv\tfrac{1}{4}[3+(9-8\epsilon)^{1/2}]$$

ϵ	E_0	r_c
1.0	4.36	2.70
0.8	5.51	1.59
0.6	6.16	1.29
0.4	6.97	1.13
0.2	7.73	1.02
0.0	8.48	0.94

is unlikely. However, including higher-order terms in the free energy introduces different length scales and a more accurate description may contain an interface.

B. Landau Theory

The solutions in the Sec. VII A give the connection between the theory for the blue phases presented here and the Landau Theory as discussed by Brazovskii, Hornreich and Shtrikman, and others. The solution in Sec. VII A is easily seen to be analytic at the center of the disclination. From the variation equations for α and β that derive from the free energy in Eq. (7.11), it is easily shown that

$$\alpha+\beta\equiv A(r)=\sum_{l=0}^{\infty}A_l r^{2l},$$

$$\alpha-\beta\equiv B(r)=r\sum_{k=0}^{\infty}B_k r^{2k}$$

$$\equiv rb(r), \tag{7.14}$$

so that A and b are analytic functions at $r=0$. Substitution of the results into Eq. (7.3) for $Q_{\alpha\beta}$ gives

$$Q=\frac{A}{2}\begin{pmatrix}\frac{1}{3}&0&0\\0&\frac{1}{3}&0\\0&0&-\frac{2}{3}\end{pmatrix}+\frac{b}{2}\begin{pmatrix}x&-y&0\\-y&-x&0\\0&0&0\end{pmatrix}. \tag{7.15}$$

Thus, $Q_{\alpha\beta}(\vec{r})$ is completely analytic at the origin. A detailed examination of the plane-wave solutions generated by Hornreich and Shtrikman for various possible symmetries reveals that they indeed have lines in the real space unit cell about which $Q_{\alpha\beta}$ varies as described by Eq. (7.15). Thus, our interpretation of their biaxial solutions is that the biaxiality is present in order to describe the core of the disclinations required to satisfy the double twist desired by chirality. Because the solutions are plane waves, the core of the disclinations is necessarily rather spread out in the unit cell. The fundamental mechanism of both approaches is the energy gain from double twist coupled to the topological impossibility of introducing double twist throughout space. The biaxiality is as much a property of disclinations in nematics as in cholesterics. It would be interesting to investigate experimentally the core of disclinations near T_c in nematics to ascertain whether the mean-field solutions presented here are correct. It is known that mean-field theory gives a rather poor description of the phase transition itself in that the magnitude of the order parameter at T_c is considerably larger than expected from extrapolations of susceptibilities in the isotropic phase. How this affects the disclination core is unclear at present.

VIII. CONCLUSIONS

A really quantitative comparison of theory and experiment is at present impractical. We lack a complete set of experimental parameters for even one cholesteric substance, and the energetics of disclinations is not well known: One cannot ascribe quantitative accuracy to either the isotropic-core model or the mean-field calculations. For the same reason, it is rather speculative to try to correlate the various blue phases that have been observed with specific symmetry structures on the basis of calculated free energy. Although a comparison of the various cases given in Figs. 5—10 shows that there can be ample opportunity for one structure to produce the lower free energy in a given temperature range, while another structure does so in an adjacent range, the balance is obviously a delicate one. Incidentally, such an explanation of the blue phase I to II transitions does predict a first-order transition, as is indeed observed.[5]

The calculations presented clearly indicate that the structures discussed are possible stable crystalline structures. From the group-theoretical analysis of Hornreich and Shtrikman one concludes that the three examined here are the most likely ones to occur. Within our parametrization scheme, the O^2 and O^8 structures appear somewhat lower in free energy than O^5. The two are therefore the best possibilities for the BPI and BPII.

Note added in proof. (1). A detailed description of the computer program is given in Ref. 27. (2). We have recently treated a new structure with O^8 symmetry, obtained by reversing the sign of the tensorial order parameter of the present O^8 structure. Computation gives a lower free energy for the new structure, compared to the one reported here.

ACKNOWLEDGMENTS

We wish to acknowledge continuing advice and help in computer programming by D. W. Berreman. Thanks are also due to H. S. Greenside for help with the Schryer programs.

[1]H. Stegemeyer and K. Bergmann, in *Liquid Crystals of One- and Two-Dimensional Order,* proceedings of the Garmisch-Partenkirchen Conference, 1980, edited by W. Helfrich and G. Heppke (Springer, New York, 1980), p. 161.

[2]A. Saupe, Mol. Cryst. Liq. Cryst. 7, 59 (1969).

[3]D. L. Johnson, J. H. Flack, and P. P. Crooker, Phys. Rev. Lett. 45, 641 (1980).

[4]M. Marcus, J. Phys. (Paris) 42, 61 (1981).

[5]S. Meiboom and M. Sammon, Phys. Rev. Lett. 44, 882 (1980); Phys. Rev. A 24, 468 (1981).

[6]A. J. Nicastro Ph.D. thesis, University of Delaware, 1981 (unpublished).

[7]S. A. Brazovskii and S. G. Dmitriev, Zh. Eksp. Teor. Fiz. 69, 979 (1975) [Sov. Phys.—JETP 42, 497 (1976)].

[8]S. A. Brazovskii and V. M. Filev, Zh. Eksp. Teor. Fiz. 75, 1140 (1978) [Sov. Phys.—JETP 48, 573 (1978)].

[9]S. Alexander, in *Symmetries and Broken Symmetries in Condensed Matter Physics, Proceedings Colloque Pierre Curie, 1980,* edited by N. Boccara (Inst. Dev. Sci. Educ. Technol., Paris, 1981).

[10]R. M. Hornreich and S. Shtrikman, J. Phys. (Paris) 41, 335 (1980); also in *Liquid Crystals of One- and Two-Dimensional Order,* proceedings of the Garmisch-Partenkirchen Conference, edited by W. Helfrich and G. Heppke (Springer, New York, 1980), p. 185.

[11]R. M. Hornreich and S. Shtrikman Phys. Lett. 84A, 20 (1981); Phys. Rev. A 24, 635 (1981).

[12]R. M. Hornreich and S. Shtrikman, Phys. Lett. 82A, 354 (1981).

[13]S. Meiboom, J. P. Sethna, P. W. Anderson, and W. F. Brinkman, Phys. Rev. Lett. 46, 1216 (1981).

[14]This equation can be obtained from the more general one of Ref. 7 by substituting $Q_{\alpha\beta}=(n_\alpha n_\beta-\frac{1}{3}\delta_{\alpha\beta})$. Alternatively, the first term is given in Ref. 15 for nematics and it can be shown that the second term is the appropriate one for the cholesteric twist.

[15]P. G. de Gennes, *The Physics of Liquid Crystals* (Clarendon, Oxford, 1975), p. 67.

[16]J. Nehring and A. Saupe, J. Chem. Phys. 54, 337 (1971).

[17]We have chosen this definition for the sake of simplicity. Alternatively we could have chosen an effective R which makes the volume of the disclination core equal to the volume of the excluded cubes. Disregarding the disclination crossings in the O^5 and O^2 structures, this assumption would give for O^8: $R_{\text{eff}}=(4/\pi)(d/N)$, and for O^5 and O^2: $R_{\text{eff}}=[7/(\pi\sqrt{3})](d/N)$.

[18]P. G. de Gennes, Ref. 15, p. 131.

[19]Near a first-order transition, the free energy as function of temperature for the two phases is given by two lines intersecting at T_c. We use the relation $(\partial G/\partial T)_p=-S$, where G is the Gibbs free energy, and approximate the lines near T_c by straight sections. Applying this equation to both the isotropic and cholesteric phases, and taking the difference, we obtain for the entropy of transition $\Delta S=(G_{\text{iso}}-G_{\text{chol}})/(T_c-T)$. A typical value of ΔS is 8×10^4 ergs cm^{-3} K^{-1}. See, for instance, E. M. Barrall and J. F. Johnson, in *Liquid Crystals and Plastic Crystals,* edited by G. W. Gray and P. A. Winsor (Wiley, New York, 1974), Vol. II, p. 254.

[20]Recent references that can provide a key to earlier ones are as follows: Hp. Schad and M. A. Osman, J. Chem. Phys. 75, 880 (1981); F. Leenhouts and A. J. Dekker, J. Chem. Phys. 74, 1956 (1981). These papers report work on nematics. We have not found any measurements on cholesterics.

[21]M. Kahlweit and W. Ostner, Chem. Phys. Lett. 18, 589 (1973).

[22]D. Langevin and M. A. Bouchiat, Mol. Cryst. Liq. Cryst. 22, 317 (1973); C. R. Acad. Sci. Ser. B 227, 731 (1973).

[23]D. Demus, H.-G. Hahn, and F. Kuschel, Mol. Cryst. Liq. Cryst. 44, 61 (1978).

[24]We have combined data given in Figs. 2, 3, and 4 and Tables II and III of Ref. 23. These data are not completely consistent—they were presumably made on a number of different samples. We believe that our Fig. 14 is a reasonable composite.

[25]It should be noted that the existence range of the blue phase is 0.4 °C for the first case and 0.9 °C for the second. The experimental range is 0.65 °C. We have not attempted to adjust for this difference, but simply plotted results relative to the cholesteric-blue-phase transition temperature.

[26]M. Marcus and J. W. Goodby, Mol. Cryst. Liq. Cryst. Lett. 71, 297 (1982).

[27]M. Sammon, Mol. Cryst. Liq. Cryst. 89, 305 (1982).